Heliyon 5 (2019) e02384

Contents lists available at ScienceDirect

Heliyon

www.elsevier.com/locate/heliyon

# Vinyl cyanide ($CH_2CHCN$) in interstellar space: potential spectral lines for its detection

Mohit K. Sharma *

*Amity Centre for Astronomy & Astrophysics, Amity Institute of Applied Sciences, Amity University, Sector 125, Noida 201313, U.P., India*

ARTICLE INFO

*Keywords:*
Astrophysics
Radiative transfer
ISM: molecules
Vinyl cyanide
Astrobiology

ABSTRACT

Vinyl cyanide is a molecule having planar geometry with electric dipole moment components, $\mu_a = 3.821$ D and $\mu_b = 0.687$ D. Thus, *a*-type transitions are very strong as compared to *b*-type transitions, and are considered in this investigation. The rotational levels for *a*-type transitions, may be divided into two distinct groups: one group having odd values of $k_a$ and the other having even values of $k_a$. Using the known values of rotational and centrifugal distortion constant along with the electric dipole moment $\mu_a$, we have calculated energies of lower 120 rotational levels, having energy up to 92 $cm^{-1}$, for each group, and the probabilities for radiative transitions between the levels. These radiative transition probabilities in conjunction with the scaled values of collisional rate coefficients are used in the Sobolev Large Velocity Gradient analysis. Out of a large number of lines, we have selected the strongest ones. In the low lying levels, besides the 4 observed lines of $CH_2CHCN$, we have discussed about 8 additional transitions, of which 2 showing the phenomenon of anomalous absorption and 6 showing emission feature are found. These lines may play important role for the search of vinyl cyanide in a cosmic object.

## 1. Introduction

Vinyl cyanide ($CH_2CHCN$), also known as the acrylonitrile or propenenitrile, may be the best candidate for the formation of cell-like membranes in Titan's hydrocarbon-rich lakes and seas [1]. Lai et al. [2] have performed the first spatial distribution mapping of $CH_2CHCN$ in the atmosphere of Titan with the help of ALMA. Along with $C_2H_5CN$, $HC_3N$ and $CH_3CN$, the new maps of $CH_2CHCN$ has been spatially resolved on Titan and their abundances are derived using the radiative transfer modeling.

Outside the solar system, it is discovered towards the galactic center in Sgr B2 by Gardner & Winnewisser [3] through its transition $2_{11}$–$2_{12}$ at 1.372 GHz, in dense dark cloud TMC-1 by Matthews & Sears [4] and in carbon-rich star IRC +10216 by Agundez et al. [5]. Lopez et al. [8] detected vinyl cyanide in Orion-KL with IRAM-30 m in the frequency range between 80–280 GHz in its ground and vibrationally excited states. Because of its importance, laboratory spectrum of $CH_2CHCN$ is studied from time to time [6, 7, 8]. The rotational and centrifugal distortional constants derived by Lopez et al. [8] in $I^r$ representation, with Watson A-reduction Hamiltonian are given in Table 1, and are used in the present investigation. Vinyl cyanide is a planar molecule whose components of electric dipole moment, $\mu_a = 3.815$ D and $\mu_b = 0.894$ D were obtained by Stolze & Sutter [9] which are modified to be $\mu_a = 3.821$ D and $\mu_b = 0.687$ D by Krasnicki & Kisiel [10], showing that its *a*-type transitions are very strong as compared to the *b*-type transitions. Thus, in the present investigation, we have considered *a*-type transitions. The vinylcyanide may be produced by a reaction of propylene, ammonia and oxygen

$$CH_2 = CH\text{-}CH_3 + NH_3 + 1.5\ O_2 \longrightarrow CH_2 = CH - CN + 3H_2O \quad (1)$$

The rotational levels for *a*-type transitions, may be classified into two distinct groups: one group having odd values of $k_a$ and the other having even values of $k_a$. There are no radiative as well as collisional transitions between the levels of these groups. Using the rotational and centrifugal distortion constants given in Table 1, and electric dipole moment $\mu_a$, for each group, we have calculated energies of 120 lower rotational levels, having energy up to 92 $cm^{-1}$, and the Einstein coefficients for radiative transitions between the levels with the help of ASROT [11]. These radiative transition probabilities in conjunction with the scaled values of collisional rate coefficients are used for solving the statistical equilibrium equations coupled with the equations of radiative transfer.

* Corresponding author.
*E-mail addresses:* mohitkumarsharma32@yahoo.in, mksharma4@amity.edu.

https://doi.org/10.1016/j.heliyon.2019.e02384
Received 11 April 2019; Received in revised form 21 June 2019; Accepted 23 August 2019

**Table 1**
Rotational and centrifugal distortion constants.

| Constant | Value (MHz) | Constant | Value (MHz) |
|---|---|---|---|
| $A$ | 49850.69655 | $\phi_K$ | $3.7011 \times 10^{-5}$ |
| $B$ | 4971.212565 | $L_J$ | $-2.6315 \times 10^{-14}$ |
| $C$ | 4513.828526 | $L_{JJK}$ | $-1.077 \times 10^{-12}$ |
| $\Delta_J$ | $2.244058 \times 10^{-3}$ | $L_{JK}$ | $4.279 \times 10^{-10}$ |
| $\Delta_{JK}$ | $-8.56209 \times 10^{-2}$ | $L_{KKJ}$ | $1.2 \times 10^{-11}$ |
| $\Delta_K$ | 2.7154213 | $L_K$ | $-6.141 \times 10^{-8}$ |
| $\delta_J$ | $4.566499 \times 10^{-4}$ | $l_J$ | $-1.1602 \times 10^{-14}$ |
| $\delta_K$ | $2.44935 \times 10^{-4}$ | $l_{JK}$ | $-9.56 \times 10^{-13}$ |
| $\Phi_J$ | $6.4338 \times 10^{-6}$ | $l_{KJ}$ | $-1.436 \times 10^{-10}$ |
| $\Phi_{JK}$ | $-4.25 \times 10^{-9}$ | $l_K$ | $8.91 \times 10^{-9}$ |
| $\Phi_{KJ}$ | $-7.7804 \times 10^{-6}$ | $P_{KJ}$ | $-1.56 \times 10^{-14}$ |
| $\Phi_K$ | $3.84762 \times 10^{-4}$ | $P_{KKJ}$ | $-1.977 \times 10^{-13}$ |
| $\phi_J$ | $2.36953 \times 10^{-9}$ | $P_K$ | $8.67 \times 10^{-12}$ |
| $\phi_{JK}$ | $1.4283 \times 10^{-7}$ | | |

In the low lying levels, besides the 4 observed lines of $CH_2CHCN$, we have discussed about 8 additional transitions, of which 2 are found to show anomalous absorption and 6 are found to show emission feature. These lines may play important role in the search of vinyl cyanide in a cosmic object. The transitions observed by Agundez et al. [5] are between higher levels, and 10 out of them are analyzed here.

## 2. Model

In the Sobolev Large Velocity Gradient (LVG) analysis, discussed in Sharma [16] and Sharma et al. [17], we have solved a set of statistical equilibrium equations coupled with the equations of radiative transfer. The required input data in the analysis are the radiative transition probability (Einstein $A$ and $B$ coefficients) discussed in section 2.2 and the collisional rate coefficients, discussed in section 2.3. The set of equations is solved through iterative method where initial population densities are taken as thermal ones.

### 2.1. Rotational levels

In a cosmic object where vinyl cyanide may be found, the kinetic temperature may be few tens of Kelvin, and thus, we are concerned with the rotational levels in the ground vibrational state and ground electronic state. For an asymmetric top molecule, $J_{k_a k_c}$ is the rotational level where $J$ is the rotational quantum number, and $k_a$ and $k_c$ denotes the projections of $J$ on the axis of symmetry in case of the prolate and oblate symmetric tops, respectively. These levels are connected through radiative as well as collisional transitions.

### 2.2. Radiative transitions

The electric dipole moment of vinyl cyanide has the components $\mu_a = 3.821$ Debye and $\mu_b = 0.687$ Debye, showing that its $a$-type transitions are much intense as compared to the $b$-types. In our calculations, we have considered only $a$-type transitions, governed by the selection rules:

$$J: \quad \Delta J = 0, \pm 1$$

$$k_a, k_c: \quad \text{odd, even} \longleftrightarrow \text{odd, odd} \qquad \text{(group I)}$$

$$\text{even, even} \longleftrightarrow \text{even, odd} \qquad \text{(group II)}$$

The levels in group I have odd value of $k_a$ whereas in group II have even value of $k_a$. Between 120 levels, there are 393 and 405 radiative transitions, for the groups I and II, respectively. We have calculated radiative transition probabilities between the levels, using the rotational and centrifugal distortion constants given in Table 1, with the help of the software ASROT [11].

### 2.3. Collisional transitions

Besides the radiative transitions, the levels are connected through the collisional transitions due to collisions with the molecular hydrogen $H_2$, which is the most abundant in a molecular region. In the study of interstellar molecules, the calculation of collisional rate coefficients is the most difficult part [12, 13, 14] as collisional transitions do not follow any selection rules. The collisional rate coefficients for one direction (excitation or deexcitation) of the transitions has to be calculated, as the collisional rate coefficients for the reverse direction can be calculated with the help of the detailed equilibrium [15]. Collisional rate coefficients are not available for the vinyl cyanide. In absence of the collisional rate coefficients, the deexcitation rate coefficients for a kinetic temperature $T$ are calculated following the procedure discussed by Sharma [16] and Sharma et al. [17].

### 2.4. Anomalous absorption

Anomalous absorption is an unusual phenomenon developed under some specific condition. The required condition for brightness temperature $T_B$ of transition showing anomalous absorption is $0 < T_{ex} < T_B < T_{bg}$ (Sharma et al. [17]) where $T_{ex}$ is the excitation temperature of transition and $T_{bg}$ (= 2.73 K) is background temperature of Cosmic Microwave Background. The brightness temperature may be defined ass the temperature of a black body corresponding to the given intensity of radiation and is given by

$$T_B = \frac{h\nu}{k} \frac{1}{\ln[1 + 8\pi h\nu^3 / Ic^3]} \tag{2}$$

where $I$ is the intensity of radiation.

## 3. Results & discussion

For the kinetic temperature considered here, up to 50 K, 120 levels having energy up to 92 $cm^{-1}$, are sufficient for the LVG analysis. For each group of rotational levels, a set of 120 statistical equilibrium equations coupled with the respective equations of radiative transfer is solved with the help of iterative procedure, where the radiative transition probabilities and the collisional rate coefficients are used as input parameters. The iterative method is initiated with the thermal population densities of levels corresponding to the kinetic temperature in the region. In order to include a large number of cosmic objects, where the vinyl cyanide may be found, in the calculations, we have considered wide ranges of physical parameters. The molecular hydrogen density $n_{H_2}$ is taken from $10^2$ to $10^6$ $cm^{-3}$; the kinetic temperatures $T$ are 10, 20, 30, 40 and 50 K, values of $\gamma [= n_{mol}/(dv_r/dr)]$ are taken as $10^{-6}$ and $10^{-5}$ $cm^{-3}$ $(km/s)^{-1}$ pc. Here $n_{mol}$ denotes the density of vinyl cyanide, and $dv_r/dr$ the velocity-gradient in the region. There are large number of emission and absorption lines, we have selected the strongest ones.

Fig. 1 shows the variation of brightness temperatures $T_B$ (K) versus the molecular hydrogen density $n_{H_2}$ for the kinetic temperatures of 10, 20, 30, 40 and 50 K for six transitions of group I. The vinyl cyanide was discovered by Gardner & Winnewisser [3] through its transition $2_{11}$–$2_{12}$ at 1.372 GHz in emission towards SgrB2. This transition, we have however found to show anomalous absorption. Two transitions $2_{12}$–$1_{11}$ at 18.513 GHz and $2_{11}$–$1_{10}$ at 19.427 GHz observed by Matthews & Sears [4] in the dense dark cloud TMC-1 are found to show emission feature. Other two lines $1_{10}$–$1_{11}$ at 0.457 GHz and $3_{12}$–$3_{13}$ at 2.744 GHz are found to shows anomalous absorption, one transition $3_{12}$–$2_{11}$ at 29.139 GHz is emission line.

In Fig. 2, we have given results for 6 lines of group II. All six transitions are found to show emission feature. The line $1_{01}$–$0_{00}$ at 9.485 GHz is found as intense as the line $2_{02}$–$1_{01}$ at 18.967 GHz observed by Matthews & Sears [4] in the dense dark cloud TMC-1. Other four lines, $3_{03}$–$2_{02}$ at 28.441 GHz, $3_{21}$–$2_{20}$ at 28.471 GHz, $3_{22}$–$2_{21}$ at 28.457 GHz, $4_{04}$–$3_{03}$ at 37.905 GHz are found with emission.

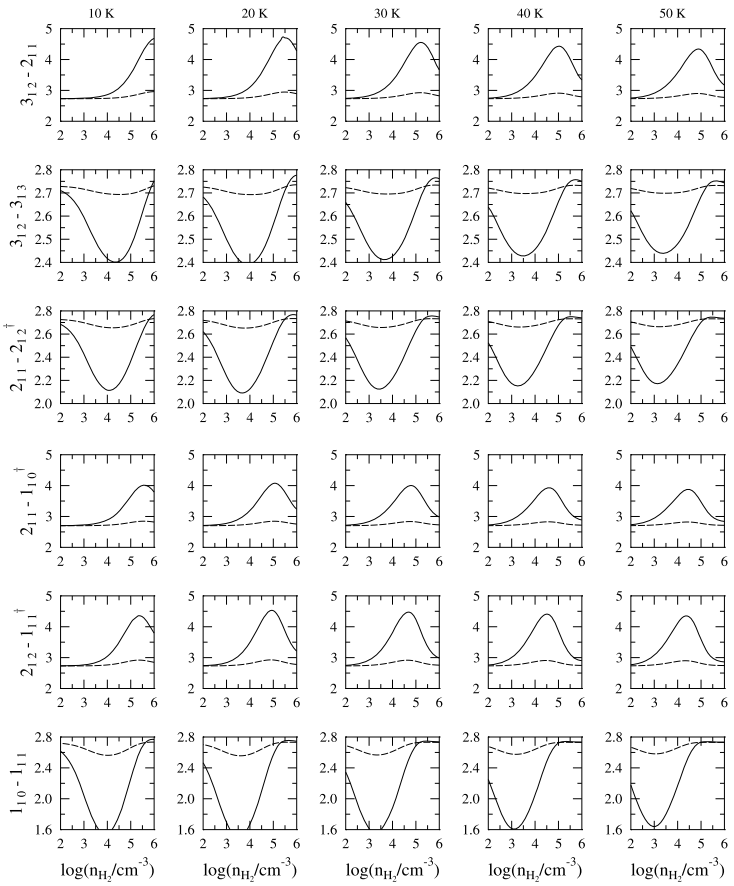


**Fig. 1.** Variation of brightness temperatures $T_B$ (K) versus molecular hydrogen density $n_{H_2}$ for kinetic temperatures of 10, 20, 30, 40 and 50 K, written at the top, for six transitions of group I, written on the left. Three transitions observed in a cosmic object are marked by the symbol †. Solid line is for $\gamma = 10^{-5}$ cm$^{-3}$ (km/s)$^{-1}$ pc, and the dotted line for $\gamma = 10^{-6}$ cm$^{-3}$ (km/s)$^{-1}$ pc.

**Table 2**
Frequency $\nu$, $A$-coefficient $A_{ul}$, energy $E_u$ of upper level, radiative life-time $t_u$ of upper level and $t_l$ of lower level for transitions.

| Transitions | $\nu$ (GHz) | $A_{ul}$ (s$^{-1}$) | $E_u$ (cm$^{-1}$) | $t_u$ (s) | $t_l$ (s) |
|---|---|---|---|---|---|
| $1_{10}$–$1_{11}$ | 0.457 | 8.125E-12 | 1.827 | 1.23E+11 | ∞ |
| $2_{12}$–$1^{\dagger}_{11}$ | 18.513 | 3.235E-07 | 2.429 | 3.09E+06 | ∞ |
| $2_{11}$–$1^{\dagger}_{10}$ | 19.427 | 3.738E-07 | 2.475 | 2.67E+06 | 1.23E+11 |
| $2_{11}$–$2^{\dagger}_{12}$ | 1.372 | 7.312E-11 | 2.475 | 2.67E+06 | 3.09E+06 |
| $3_{12}$–$3_{13}$ | 2.744 | 2.925E-11 | 3.446 | 6.24E+05 | 7.22E+05 |
| $3_{12}$–$2_{11}$ | 29.139 | 1.602E-06 | 3.446 | 6.24E+05 | 2.67E+06 |
| $1_{01}$–$0_{00}$ | 9.485 | 4.834E-08 | 0.316 | 2.07D+07 | ∞ |
| $2_{02}$–$1^{\dagger}_{01}$ | 18.967 | 4.638E-07 | 0.948 | 2.16D+06 | 2.07D+07 |
| $3_{03}$–$2_{02}$ | 28.441 | 1.675E-06 | 1.896 | 5.97D+05 | 2.16D+06 |
| $3_{21}$–$2_{20}$ | 28.471 | 9.338E-07 | 7.911 | 1.03D+06 | 7.35D+07 |
| $3_{22}$–$2_{21}$ | 28.457 | 9.324E-07 | 7.910 | 1.04D+06 | 7.83D+07 |
| $4_{04}$–$3_{03}$ | 37.905 | 4.113E-06 | 3.160 | 2.43D+05 | 5.97D+05 |

None of these lines is found to show any MASER action. With the increase of kinetic temperature, the strength of anomalous absorption is found to decrease and the position of trough is found to shift towards the low density. For the emission lines, the position of peak is found to shift towards the low density with the increase of kinetic temperature. Though the transitions $1_{10}$–$1_{11}$ and $1_{01}$–$0_{00}$ which are connecting the ground state in I and II groups are not detected in a cosmic object, but their probability for detection is quite good. These 8 transitions along with 4 observed, may play important role in the detection of vinyl cyanide in a cosmic object.

The frequency of transition, Einstein $A$-coefficient for the transition, energy of upper level, radiative life-times of upper and lower levels of the 12 transitions have been given in Table 2.

Out of the lines of $CH_2CHCN$ detected by Agundez et al. [5] in the C-rich star IRC +10216, 5 lines group I are shown in Fig. 3 and lines group II are shown Fig. 4. All these lines are found to show emission feature. The intensities of lines are found to increase with the increase of kinetic temperature (Fig. 5).

Four lines $38_{1,38}$–$37_{1,37}$, $38_{0,38}$–$37_{0,37}$, $36_{2,34}$–$35_{2,33}$ and $37_{1,36}$–$36_{1,35}$ detected by Lai et al. [2] in the atmosphere of Titan lie at very high energy and are beyond the scope of our investigation.

## 4. Conclusions

We have solved a set of statistical equilibrium equations coupled with the equations of radiative transfer for two groups of rotational levels of $CH_2CHCN$. In the lower levels, besides the 4 observed lines, 8 lines are discussed. These lines may help in detection of vinyl cyanide in a cosmic object. In particular, the detection of lines connecting the ground state is highly probable.

## Declarations

### *Author contribution statement*

Mohit K. Sharma: Conceived and designed the experiments; Performed the experiments; Analyzed and interpreted the data; Wrote the paper.

### *Funding statement*

This research did not receive any specific grant from funding agencies in the public, commercial, or not-for-profit sectors.

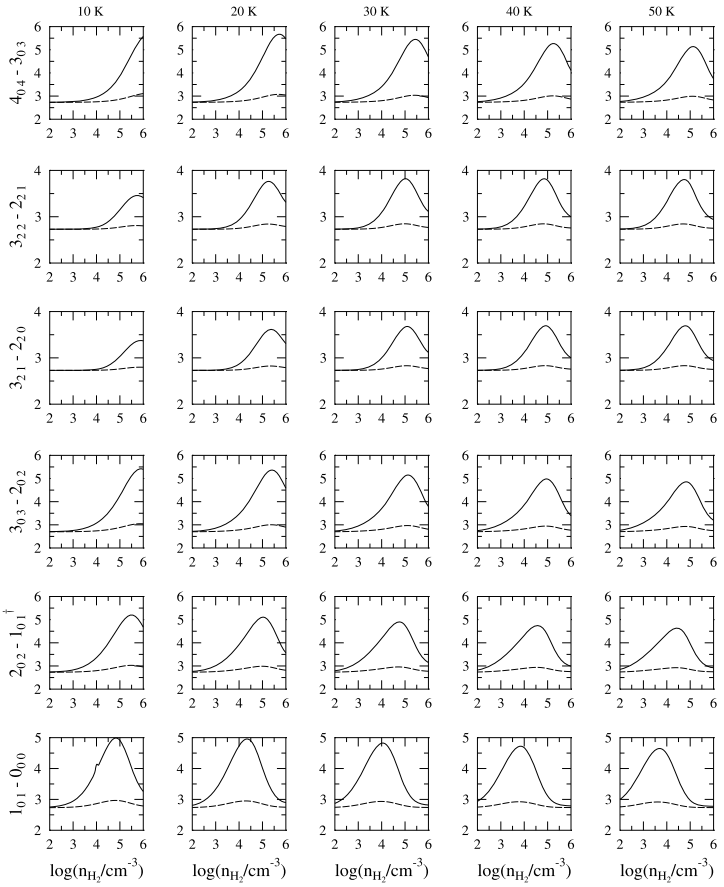


**Fig. 2.** Variation of brightness temperatures $T_B$ (K) versus molecular hydrogen density $n_{H_2}$ for kinetic temperatures of 10, 20, 30, 40 and 50 K, written at the top, for six transitions of group II, written on the left. One transitions observed in a cosmic object are marked by the symbol †. Solid line is for $\gamma = 10^{-5}$ cm$^{-3}$ (km/s)$^{-1}$ pc, and the dotted line for $\gamma = 10^{-6}$ cm$^{-3}$ (km/s)$^{-1}$ pc.

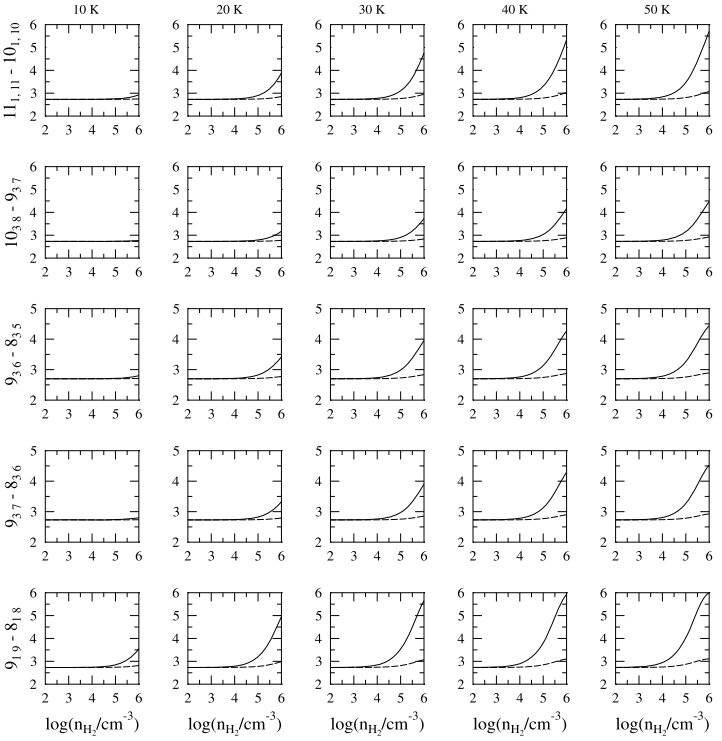


**Fig. 3.** Variation of brightness temperatures $T_B$ (K) versus molecular hydrogen density $n_{H_2}$ for kinetic temperatures of 10, 20, 30, 40 and 50 K, written at the top, for six transitions of group I, observed by Agundez et al. [5], written on the left. Solid line is for $\gamma = 10^{-5}$ cm$^{-3}$ (km/s)$^{-1}$ pc, and the dotted line for $\gamma = 10^{-6}$ cm$^{-3}$ (km/s)$^{-1}$ pc.

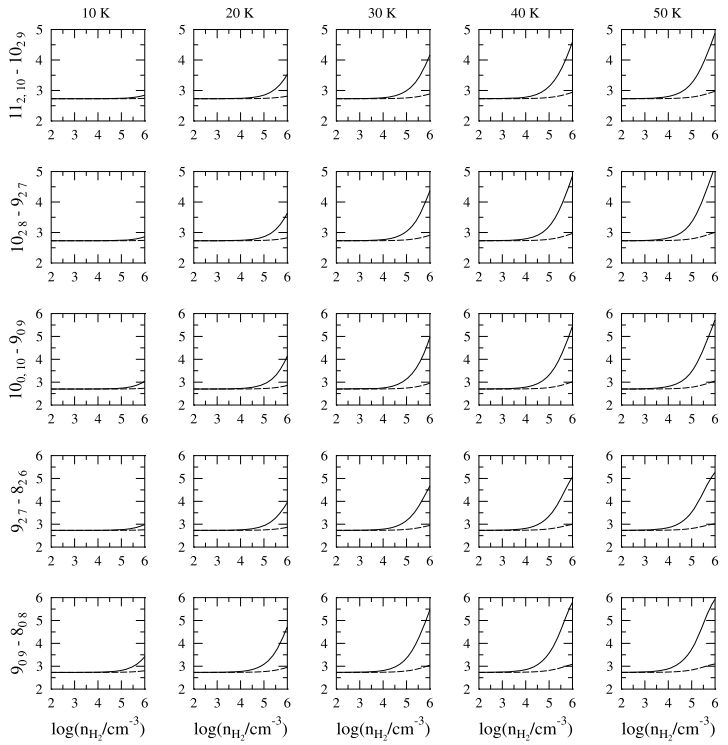


**Fig. 4.** Variation of brightness temperatures $T_B$ (K) versus molecular hydrogen density $n_{H_2}$ for kinetic temperatures of 10, 20, 30, 40 and 50 K, written at the top, for six transitions of group II, observed by Agundez et al. [5], written on the left. Solid line is for $\gamma = 10^{-5}$ cm$^{-3}$ (km/s)$^{-1}$ pc, and the dotted line for $\gamma = 10^{-6}$ cm$^{-3}$ (km/s)$^{-1}$ pc.

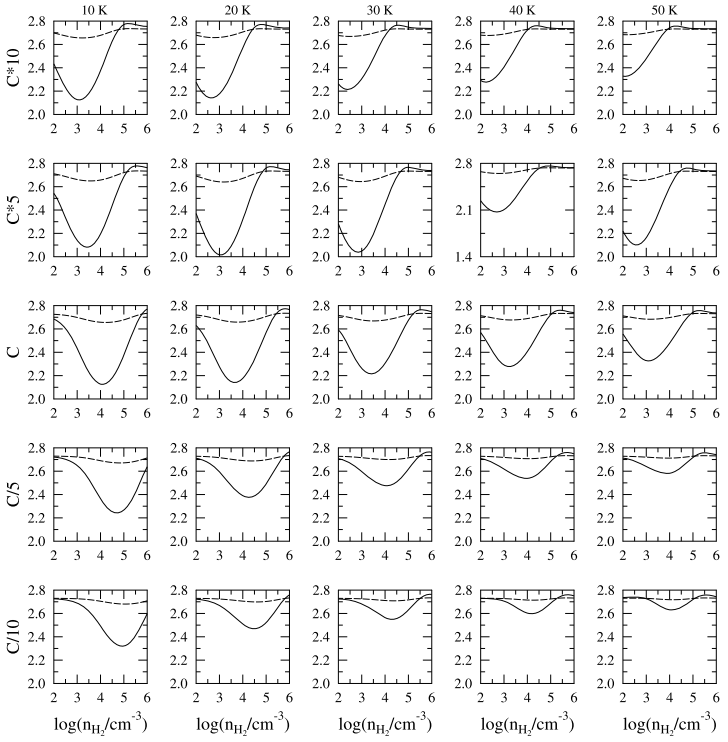


**Fig. 5.** Variation of brightness temperatures $T_B$ (K) versus molecular hydrogen density $n_{H_2}$ for kinetic temperatures of 10, 20, 30, 40 and 50 K, written at the top, for the transition $2_{11} - 2_{12}$ where collisional rate coefficients are multiplied and divided a factor 5 and 10 for the transitions with $\Delta k_a = 0$ besides the normal collisional rate coefficients. Solid line is for $\gamma = 10^{-5}$ cm$^{-3}$ (km/s)$^{-1}$ pc, and the dotted line for $\gamma = 10^{-6}$ cm$^{-3}$ (km/s)$^{-1}$ pc.

*Competing interest statement*

The authors declare no conflict of interest.

*Additional information*

No additional information is available for this paper.

**Acknowledgements**

Thanks are due to the learned reviewers for constructive comments. The author is grateful to Hon'ble Dr. Ashok K. Chauhan, Founder President, Hon'ble Dr. Atul Chauhan, Chancellor, Hon'ble Vice Chancellor Dr. Balvinder Shukla, Amity University for valuable support and encouragements.

**References**

[1] M.Y. Palmer, M.A. Cordiner, C.A. Nixon, et al., ALMA detection and astrobiological potential of vinyl cyanide on Titan, Sci. Adv. 3 (2017) e1700022–e1700027.
[2] J.C.-Y. Lai, M.A. Cordiner, C.A. Nixon, et al., Mapping vinyl cyanide and other nitriles in Titan's atmosphere using ALMA, Astrophys. J. 154 (2017) 206–2017.
[3] F.F. Gardner, G. Winnewisser, The detection of interstellar vinyl cyanide (acrylonitrile), Astrophys. J. 195 (1975) L127–L130.
[4] E. Matthews, P.J. Sears, The detection of vinyl cyanide in TMC-1, Astrophys. J. 272 (1983) 149–153.
[5] M. Agundez, J.P. Fonfria, J. Cernicharo, J.R. Pardo, M. Guelin, Detection of circumstellar $CH_2CHCN$, $CH_2CN$, $CH_3CCH$, and $H_2CS$, Astron. Astrophys. 479 (2008) 493–501.
[6] M.C.L. Gerry, G. Winnewisser, The microwave spectrum and centrifugal distortion constants of vinyl cyanide, J. Mol. Spectrosc. 48 (1973) 1–16.
[7] Z. Kisiel, L. Pszczolkowskii, B.J. Drouin, et al., The rotational spectrum of acrylonitrile to 1.67 THz, in: Int. Sym. Mol. Spect, vol. 258, 2009, pp. 26–34.
[8] A. Lopez, B. Tercero, Z. Kisiel, et al., Laboratory characterization and astrophysical detection of vibrationally excited states of vinyl cyanide in Orion-KL, Astron. Astrophys. 572 (2014) A44–A82.
[9] M. Stolze, D.H. Sutter, Molecular g-values, magnetic susceptibility anisotropics, molecular electric quadrupole moments, improved molecular electric dipole moments and $^{14}$N-quadrupole coupling constants of acrylonitrile, $H_2C = CH - CN$, and the magnetic susceptibility tensor of the nitrile group, Z. Naturforsch. A 40 (1985) 998–1010.
[10] A. Krasnicki, Z. Kisiel, Electric dipole moments of acrylonitrile and of propionitrile measured in supersonic expansion, J. Mol. Spectrosc. 270 (2011) 83–87.
[11] Z. Kisiel, J. Demasion, et al., Spectroscopy from Space, Kluwer, Dordrecht, 2001, pp. 91–106.
[12] M. Sharma, M.K. Sharma, U.P. Verma, S. Chandra, Collisional rates for rotational transitions in $H_2CO$ and their application, Adv. Space Res. 54 (2014) 252–260.
[13] M.K. Sharma, M. Sharma, U.P. Verma, S. Chandra, Collisional excitation of vinylidene ($H_2CC$), Adv. Space Res. 54 (2014) 1963–1971.
[14] M.K. Sharma, M. Sharma, U.P. Verma, S. Chandra, Collisional excitation of thioformaldehyde and silylidene, Adv. Space Res. 55 (2015) 434–439.
[15] S. Chandra, W.H. Kegel, Collisional rates for asymmetrical top molecules, Astron. Astrophys. Suppl. Ser. 142 (2000) 113–118.
[16] M.K. Sharma, Transfer of radiation in the formic acid: a precursor for amino acids, J. Astrophys. Astron. 40 (2019) 10.
[17] M.K. Sharma, M. Sharma, S. Chandra, Suggestion for the detection of TiO2 in interstellar medium, Astrophys. Space Sci. 362 (2017) 168–178.